Quantification of dynamic track stiffness using machine learning

Huang, Junhui; Yin, Xiaojie; Kaewunruen, Sakdirat

DOI:
10.1109/ACCESS.2022.3191278

Document Version
Publisher's PDF, also known as Version of record

Citation for published version (Harvard):
Huang, J, Yin, X & Kaewunruen, S 2022, 'Quantification of dynamic track stiffness using machine learning', *IEEE Access*, vol. 10, pp. 78747-78753. https://doi.org/10.1109/ACCESS.2022.3191278

IEEE Access
Multidisciplinary | Rapid Review | Open Access Journal

Received 23 June 2022, accepted 9 July 2022, date of publication 14 July 2022, date of current version 1 August 2022.

Digital Object Identifier 10.1109/ACCESS.2022.3191278

RESEARCH ARTICLE

Quantification of Dynamic Track Stiffness Using Machine Learning

JUNHUI HUANG, XIAOJIE YIN, AND SAKDIRAT KAEWUNRUEN
Department of Civil Engineering, School of Engineering, University of Birmingham, Birmingham B15 2TT, U.K.

Corresponding author: Sakdirat Kaewunruen (s.kaewunruen@bham.ac.uk)

This work was supported in part by the European Commission for H2020-Marie Skłodowska-Curie Actions (MSCA)-RISE Project "RISEN: Rail Infrastructure Systems Engineering Network" (www.risen2rail.eu) under Grant 691135; in part by the H2020 Shift2Rail Project (S-Code) under Grant 730849; in part by the Loram Maintenance of Way (LORAM); in part by the Brazilian Railway Authority; in part by the China Academy of Railway Sciences (CARS); in part by Network Rail; and in part by the Rail Safety and Standards Board (RSSB), U.K.

ABSTRACT Railway track stiffness is an essential factor influencing the track conditions and long-term deterioration. However, the traditional ways to measure the track stiffness are based on inverse computations using multi-body simulations and/or finite element models, which are time-consuming and at low-speed operation. To overcome these challenges, we propose a convolutional neural network framework to predict the track dynamic stiffness using the accelerations captured by accelerometers mounted on the axle box in real-time. To provide a benefit of computational cost-friendly, a dilated convolutional layer has been added which allows the framework to be applied to a compact device. In our study, a nonlinear finite element model of train-track interactions has been calibrated and used to generate unbiased, full range of data sets of axle box accelerations under various track and operational factors. Subsequently, the simulated data is formatted to three different sample sizes: 250-timesteps, 500-timesteps, and 1,000-time steps. The fine-tuned CNN model is developed based on the three datasets and provides the optimal R^2 of 0.94, 0.94, and 0.97. The insights gained from this study can assist the track stiffness measurement in the field with a novel measurement method providing continuous, cost-friendly, fast, and implementable benefits. The quantification of dynamic track stiffness will help track engineers to locate problematic and defective tracks promptly on the vast railway networks such as mud pumping, loss of support, pulverized ballast, and so on.

INDEX TERMS Track stiffness, axle box accelerations, dilated convolutional, machine learning, railway infrastructure.

I. INTRODUCTION

Railway track stiffness, representing the track deflection responding to the wheel load, is a vital parameter from a design and maintenance point of view. High track stiffness generally allows larger load and smaller track deflection but faster wear and fatigue rate on other track components such as rails, sleepers, and ballast. To make the railway more competitive and attractive, it is expected that higher running speed and low maintenance cost of the track as can be seen from two cases, a dated but illustrative case Marid-Barcelona high-speed line operating over 300 km/h in certain sections and an in-progress example the UK high-speed railway. From the design point of view, there has been an interest in adopting an optimum track stiffness to limit track deterioration and the cost of maintenance as evaluated in [1]. In the aspect of track maintenance, track stiffness can be an essential indicator for identifying the root cause of the track geometric problems [2]. It is noted that the optimal use of maintenance resources can be executed, leading to the best use of the maintenance budget based on the continuous measurement of the track stiffness with a proper interpretation of the result [3].

Before we dive into the methods of track stiffness measurements, we need to understand the motivation for measuring track stiffness. Studies over the past three decades have provided important information on the correlation between

The associate editor coordinating the review of this manuscript and approving it for publication was Liangxiu Han.

track stiffness and track conditions [3], [4]. Wang *et al.* have summarized the interpretation of the track stiffness based on low track stiffness, changing stiffness in the transition zone, virtual track stiffness, and assortative stiffness [5].

The measurement of track stiffness generally refers to the global track stiffness measurement which includes all the layers of the track structure [6]. The component level stiffness, such as ballast and fastener, can be performed in the lab condition [7]. It is noticeable that the methods of track stiffness measurement have noticeably increased. Several systematic reviews of the ways of track stiffness measurement have been undertaken, such as rolling stiffness measurement vehicle [8], the hammer method [9], [10], portancemetre [11], TTCI (Transportation Technology Center, Inc) [12], FWD (Falling Weight Deflectormeter) [13], CARS (China Academy of Railway Sciences) [14], and SBB(Swiss Federal Railways) [8]. To analyze the performance of the measurements, multiple parametric studies of the obstructiveness and measurement speed are carried out. Most of the approaches aforementioned are subjected to low measurement speed with the highest speed of 60 km/h achieved by CARS. The low measure speed can lead to an additional burden on the track capacity. Considering the track stiffness measurement on the faster measurement speed, a new solution to measure global track stiffness offering benefits of continuous, wide-coverage, non-intrusive, realistic speed and load is needed. Driven by the development of the sensor and wireless communication capability, the deployment of in-service trains makes the above benefits possible. Research on using in-service trains carried out to date implemented vehicle-track dynamic interaction and the cross-entropy optimization to determine the track stiffness [15]. A numerical validation using a half-bogie model and a beam-on-elastic-foundation tack with no irregularities was provided. However, it is noted that various types of vehicles and track and track irregularities should be considered to make the framework more rigorous. Mehrali *et al.* proposed a measuring vehicle mounted with cameras and two lasers to determine track stiffness at speed up to 120 km/h [16]. The high speed allows the solution deployed to in-service trains, but we consider that the complexity of cameras and lasers usage can be reduced.

To the best of our knowledge, we are the first to adopt dilated convolutions to evaluate global track stiffness using the train axle box vibration. Such technique is justified to be suitable for the project using sensory data which presents noisy and relatively big. The sensor sometime is so sensitive that introducing too much noise therefore the dilated technique allows the model to capture the pattern from a broad field avoiding misled by the very detail but can be noise information. Another advantage the technique brings is that it reduces the computationally demanding. A validated simulation application D-track is used to generate the vibration as the input to the model. The core contributions of this framework are presented as follows.

1. A sensible CNN architecture is proposed to address vibration data. A dilated convolutional layer is introduced to provide a broad view of the input with no additional parameters. The comparative analysis between traditional CNN and the dilated CNN is provided in terms of performance and computational cost.
2. The proposed model provides robust performance as the vibration is very close to reality with the track irregularity added in the simulation stage. To visualize how the model acts between contexts with and without irregularity, three rail irregularities: dipped joint, dipped weld, and corrugation are considered in the simulation only when the track stiffness is: 100 MN/m, 600 MN/m, or 800 MN/m.
3. Our solution's main feature is inexpensive and easy installation needed since only accelerators are mounted on the axle box. This allows easy rebuilding on an in-service train to provide non-destructive, continuous, and real-time measurement.

The remainder of this paper is organized as follows. In Section 2, methodologies of D-track and the dilated CNN model are presented. Section 3 describes the results obtained by the models for the three different datasets with varied window sizes. The results are also discussed and compared with the present counterparts in this section. The final section summarizes the findings and the significance of the current study. Besides, the limitation and a hint to direct future improvement are also presented

II. METHODOLOGIES

This section starts with a description of the D-track and subsequently elaborates on how the model is developed and evaluated.

A. NONLINEAR FINITE ELEMENT SIMULATIONS

The proposed CNN model is developed using the axle box accelerations generated by a nonlinear finite element simulation package D-track, which has first been developed by Cai [17]. D-track was designed based on an ideal rail track model presented in FIGURE 1(a) which considers the rails and ties as two elastic beams. The rails are carried by the ties via the rail pads and fastening mechanism above the ties and the ballast and subgrade beneath the ties. FIGURE 2(b) presents concrete ties which can be non-uniform.

To make the rail elements more stable, two spring stiffness at each end of the rail span are used to demonstrate the mass inertial effects, flexural, and resilience of the rail support components which are presented in FIGURE 2. Cai [17] has simplified one span of the rail track to a uniform rail beam segment which is held up by two spring coefficients $\hat{K}_e$ shown in FIGURE 2 given by

$$\widehat{\boldsymbol{K}}_{\boldsymbol{e}} = \frac{K_p}{1 + \boldsymbol{k_p} \sum_{n=1}^{z} \frac{2[z_{n(d_r)}]^2}{(w_n^2 - \Omega^2) M_n}} \tag{1}$$

where k_p is the contact stiffness between two beams in FIGURE 1, z_n represents the n_{th} mode of the tie beam,

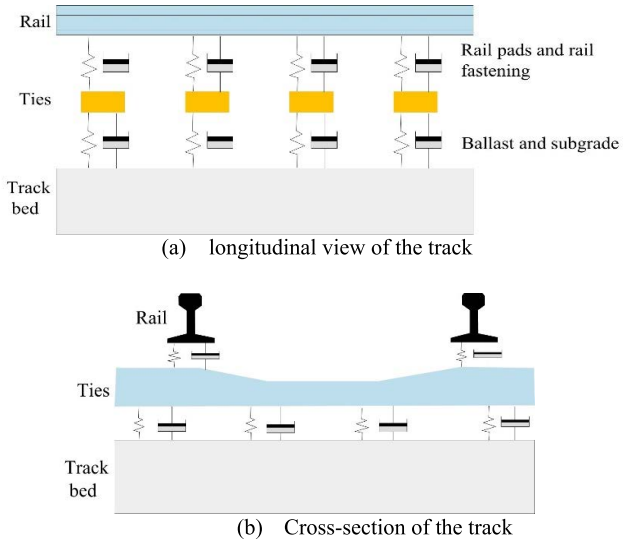

FIGURE 1. Idealized track vibration model.

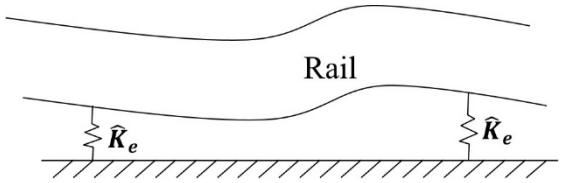

FIGURE 2. Uniform rail beam segment.

d_r reflects the distance between the end of the tie and the rail seat, Ω is the vibration frequency of the track, w_n is the natural frequency of the single free tie, and M_n stands for the tie mass.

The spring coefficient defined in (1) has been combined with the exact dynamic stiffness matrix of the rail span which is given by the following equation.

$$[K_r] = \begin{matrix} k_{11}+K_e & k_{12} & k_{13} & k_{14} \\ k_{21} & k_{22} & k_{23} & k_{24} \\ k_{31} & k_{32} & k_{33}+\widehat{K}_e & k_{34} \\ k_{41} & k_{42} & k_{43} & k_{44} \end{matrix} \tag{2}$$

With the details of each element in (2) has been unveiled in [17], the displacements responding to the nodal forces become (3) blow.

$$\{F\} = [K_r(\Omega)]\{\delta_r\} \tag{3}$$

Using (2)–(3), D-track is able to assemble the track elements and the adjacent rail span elements.

Steffens [18] has introduced the dynamic analysis of rail track structure and an interface to D-track. However, D-track's accuracy remained questionable since there was a considerable gap between the site field data and the simulated data. To boost the performance of the D-track, Leong [19] thoroughly studied the D-track in terms of sleeper pad reaction, wheel-track interaction, sleeper bending assessment. The simulated app was validated with a comparative analysis between the site data acquired from Melbourne to Geelong, Australia, and the simulated data concluded a leap of performance with less than 10% error was achieved.

TABLE 1. Parameters used in D-track.

Parameters	Value
Global Stiffness	0 - 900 MN/m
Global Damping	0 - 500 kN·s/m
Rail Type	AS60
Gauge	Standard (1435mm)
Pad/Plate Type	HDPE
Sleeper Type	Prestressed
Vehicle Speed	60-120 km/h
Vehicle Type	106t Coal Wagon
Bogie Type	QR56
Wheel Type	QR
Centre of Irregularity	Midspan Before Sleeper
Rail Analysis Position	Above Sleeper
Sleeper Analysis Position	Rail Seat
Track Modulus	12.8-41.4 Mpa m/s^2
Track irregularities	1000 mm length
	1-10 mm depth

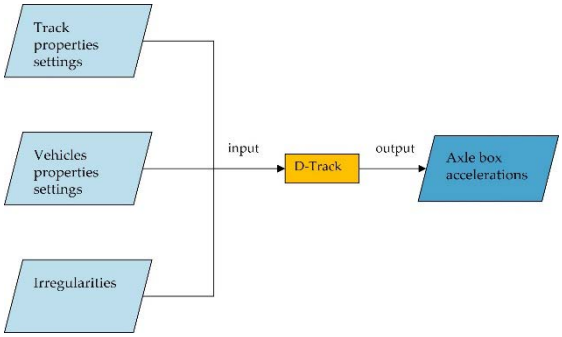

FIGURE 3. The flowchart of the D-track simulation.

D-track provides a wide range of parameters tunable such as track (global track damping and stiffness) and vehicle characteristics (models, speed, weight, and wheel radius), irregularities (dipped joint, corrugation, etc.). FIGURE 3 presents the primary procedure to generate the axle box accelerations using D-track. TABLE 1 demonstrates the details of the three inputs we tune in the simulation. As can be seen, the vehicle is running at 60 – 120 km/h in the simulation. Three track irregularities, corrugation, dip welded, and dip joint, are added to make the simulation more realistic. Prestressed sleeper, a commonly used type of sleeper, has gained popularity due to the longer life cycle and lower maintenance cost than the reinforced concrete sleeper [20]. Different stiffnesses ranging from 0 to 900 MN/m with a 100-step increase are applied. In total, 401 simulations have been executed, and the axle box accelerations corresponding to each simulation are exported to 401 excel files.

FIGURE 4 exemplifies the global vertical acceleration with the track stiffness of 300 MN/m at speeds of 60 km/h and 80 km/h. The horizontal axis represents the time step that the vibration is recorded, while the vertical axis illustrates the vertical vibration using the positive and negative values

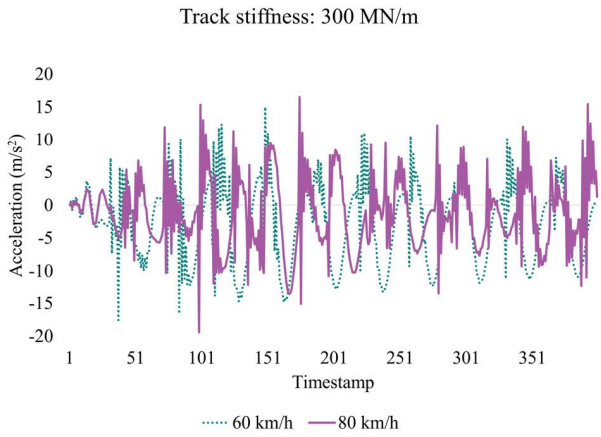

FIGURE 4. An example of the raw.

TABLE 2. The summary of the three datasets.

Window size	The number of samples
250	1604
500	802
1,000	401

to show the direction of up and down. FIGURE 4 presents two significantly different vibration patterns induced by two different speeds but pointing to the same track stiffness. The primary focus of our research has been on how we adjust the CNN model to predict the same track stiffness from two different vibration patterns. There is a possible solution that we can pre-define some hand-crafted features which are able to let the CNN group the two very different patterns in FIGURE 4 to the same track stiffness. The performance of such a design highly relies on the selection of hand-crafted features. This scenario applies to the domain where human experts can manually extract the features [21]. The summary of the three datasets is shown in TABLE 2. One Excel file is a sample using the window size of 1,000. As the window size decreases, the number of samples increases.

B. MODEL DEVELOPMENT

As aforementioned, using pre-defined hand-crafted features is notoriously difficult, not least because of the hardness of selecting the features and the human biases when defining the features. This argument has been further proven by [22], concluding that the CNN using vibration data shows superior performance compared to the deployment of the deep neural network with the handcrafted features. Vibration-based machine learning models have been thriving and used in various aspects such as structural damage monitoring [23] and railway track condition monitoring [24]. It is noted that the different machine learning models using vibration provide elegant performance and robustness in the three studies [22]–[24]. To avoid using handcrafted features, we introduce the dilated CNN model to estimate the track stiffness due to the benefits of the automatic feature extraction and the high

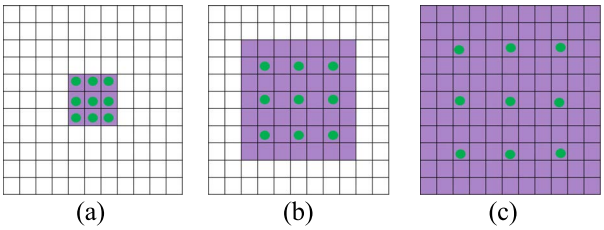

FIGURE 5. The expanded receptive field of a 3 × 3 kernel using different dilated rate l. (a) l = 1 (traditional CNN) (b) l = 2 (c) l = 3.

efficiency compared to Artificial Neural Networks(ANN) [25], especially with the raw data a bigger size than the handcrafted dataset.

1) DATA PRE-PROCESSING

Before we can input the axle box vibration to the model, data preparations, including data slicing, normalization, and splitting, must be done. Banos *et al.* have thoroughly examined the effect of data segmentation on the human activity recognition process [26]. However, we argue that the vibration pattern induced by trains entirely differs from the vibration triggered by human activity. Therefore, the impact of the window size (250, 500, and 1,000) has been evaluated in our study. Before the dataset is divided into 85% of the training set and 15% of the test set, the raw data is sliced to 250-, 500-, or 1,000-time steps per sample. 20% of the training set is split to be the validation set to achieve the model selection with no touch on the testing set during the model training and selection processes. Subsequently, the min-max normalization technique is deployed since the effectiveness has been revealed by [27]. The min-max normalization has been applied using the maximum and minimum values of the training set instead of the max and min values of the whole dataset to avoid information leaking from the test set to the training set. If we treat the test set as the future value to test a trained model, the test data's maximum and minimum are not available now.

2) DILATED CNN

Dilated convolution also known as atrous convolution, effectively enlarges the filter's receptive view along with no additional computation or the number of parameters. It has been widely used in semanticimage segmentation such as [28]. In general, the traditional convolutional layer is expanded to the dilated convolutional layer by intercalating one or more voids between the adjacent elements. Apart from sematic image segmentation, this technique has also been extended to other domains such as speech emotion recognition [29] and image classification [30].FIGURE 5 explains how dilated convolution expands the receptive field with no additional parameter introduced.

The kernel size for FIGURE 5(a) – (b) remains the same 3 × 3 (greed dots), but the receptive field differs in different size depending on the dilated rate. As can be seen, the 1-dilated convolution yields 3 × 3 receptive fields as the kernel size. Intercalating 1 zero hole around each green

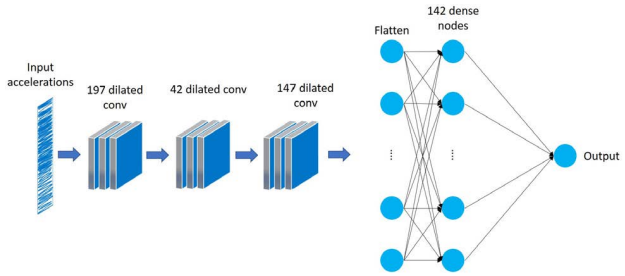

FIGURE 6. The architecture of dilated CNN.

TABLE 3. The tuned hyperparameters.

Index	Hyperparameter
A	The number of convolutional filters
B	The size of the dense layers
C	The dropout rates
D	Learning rate
E	Batch size
F	Activation function
G	Optimizer
H	Momentum

dot turns FIGURE 5(a) to (b) and the receptive field is enlarged to 7×7. The 3-dilated convolution presents an 11×11 receptive domains, as seen in FIGURE 5(c). It is noticeable that the receptive area is exponentially expanded by the dilated rate.

FIGURE 6 unfolds the architecture of the CNN using dilated techniques for the window size of 1,000. Three clusters of dilated convolutional layers can be seen followed by a flattened layer and a dense layer before the dilated CNN model predict the track stiffness. Motivated by [31], the max-pooling layer is replaced with the dilated convolutional layer to alleviate the high-frequency, high-amplitude activations. Besides, to allow the model to cover all the features, the dilated rate is suggested to be set to (1, 2, 5).

3) HYPERPARAMETER OPTIMIZATION

The weight and bias in each neuron are gained by the training process of the model. Apart from the learned parameters, the parameter, namely hyperparameter (which can be tuned manually), aims to control the learning process of the model yielding the optimal result to solve specific problems. Traditionally, the optimal scenario of hyper-parameter is decided by manual tuning. Presently, advanced GPU processors and computer clusters allow many trials with the potential hyper-parameter pre-defined, referring to grid search. The tuned hyperparameters are summarized in TABLE 3.

III. RESULT

This section presents the optimal results for both traditional CNN and dilated CNN using the test set associated with three different datasets depending on the sample size. The optimal hyperparameters are tabulated in TABLE 4 in Appendix. The mean absolute error (MAE) and the coefficient of

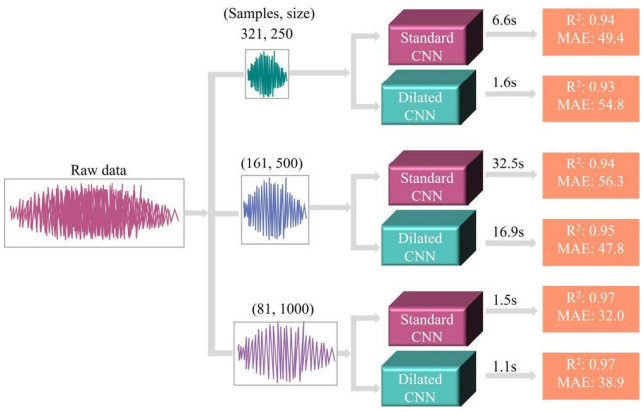

FIGURE 7. Overview of the testing result.

determination referring to R^2 are used to score the model's performance. FIGURE 7 summarizes the result for both models in terms of the performance and the time used. All the models can provide more than 90% R^2 with the peak R^2 values procured by the models using a 1000-window size. The performance between the standard CNN and dilated CNN presents almost no difference in our case; however, the dilated technique offers 75%, 45%, and 27% less time for the window size of 250, 500, and 1000. Even 27% can be dominant as the railway network is generally extensive and energy demanding.

What stands out from FIGURE 8 is that all three fine-tuned models provide promising results and less than 50 MN/m error provided by the utilization of 1,000 window size. Strong evidence of the model's performance is not sensitive to the irregularities can be found in three window size settings. It is noted that there is no additional error occurred due to the three track irregularities introduced in the track stiffnesses of 100 MN/m, 600 MN/m, and 800 MN/m compared to other track stiffness without irregularity involved. To access the effect of speed, FIGURE 8 also uses speed as x-axis to present the performance of the models. Four blocks can be seen which represent four different speed settings. By comparing the scatter of the four blocks, there is no larger gap between the performance of either dilated or non-dilated CNN due to the large speed. FIGURE 8 reflects that the main error comes from the high track stiffness error of 700 MN/m to 900 MN/m. The model presents an unfulfilled performance in the high track stiffness region, either overpredicting for the 700 MN/m or underpredicting for 800 MN/m and 900 MN/m. One possible rationale is that the vibration pattern is not sensitive to the change of the track stiffness when the value turns to a very high value like 700 MN/m to 900 MN/m. A potential solution for this can be introducing more features such as acoustics and angular velocity to assist prediction. We argue that these high stiffnesses are not common as the optimum track stiffness proposed by [32]–[34] is 70 MN/m – 130 MN/m. As aforementioned, the proposed framework allows easy refit to the service trains without causing any disruption to the daily service. Besides, our unprecedented study supports continuous, fast and cheap

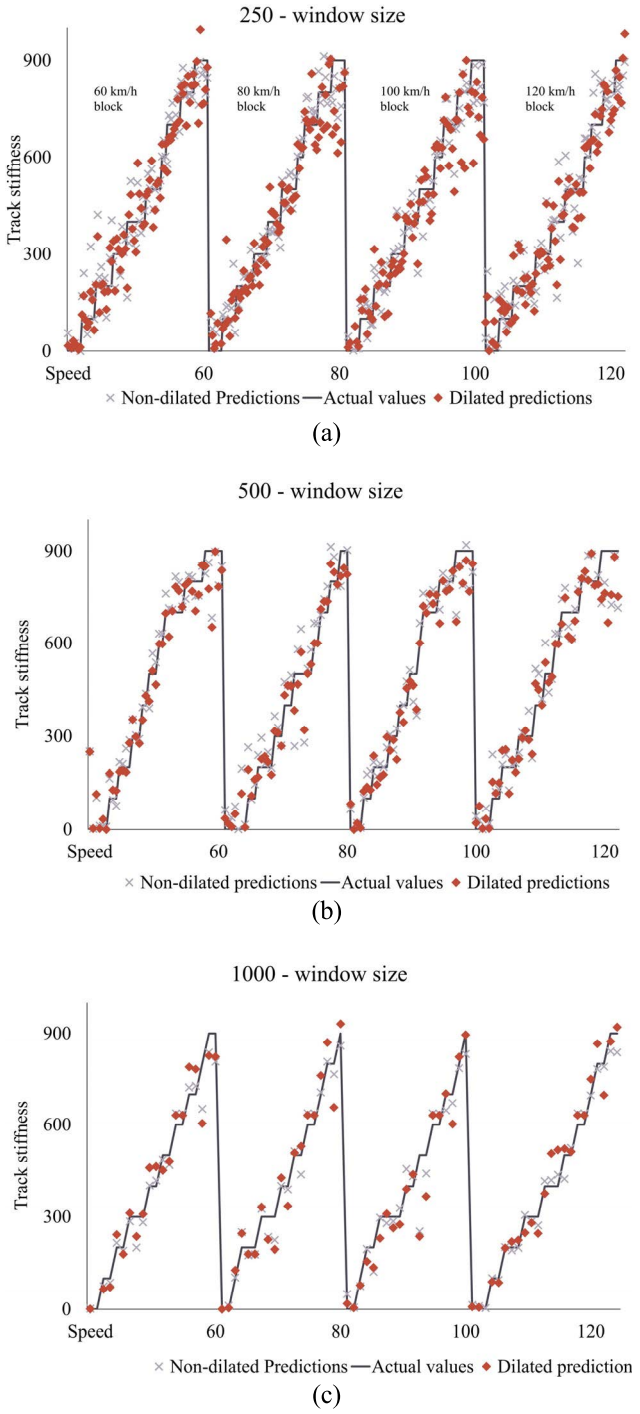

FIGURE 8. Actual values vs predictions for three dataset (a) 250 (b) 500 (c) 1000.

measurement of the track stiffness compared to the rolling stiffness measurement vehicle costs 7,000 Euro/day excluding transport to site and locomotive during measurement and the track loading vehicle costs 4,000 Euro/day excluding data evaluation, transport to site and locomotive during measurement.

As mentioned in the literature review, prior studies have reviewed the ways which are considered to be destructive and relative low speed. To tackle these constraints, Mehrali et al utilized lasers and cameras to investigate track geometry and stiffness variation [16]. However, bad weather conditions and speeds up to 120 km/h can hinder the quality of pictures taken by the camera. In our study, we have proposed a dilated CNN using the sensory data acquired from axle box which is immune to speed up to 120 km/h and bad weather conditions as there are sophisticated accelerometers designed to tackle the extreme weather conditions.

IV. CONCLUSION

This study is set out to propose a machine learning model to address the real-time global track stiffness estimation. We have confirmed that the performance of the proposed model is satisfied, the dilated technique contributes to saving computational cost, and the consideration of irregularities makes no significant difference to the model's performance. An implication of this study is the possibility that wireless accelerometers can be mounted on the axle box of the service trains. Subsequently, the vibration captured from the accelerometers can be sent to the train operation center or saved with a built-in appliance for later use by the dilated CNN model. With the continuous monitoring of track stiffness indicating the condition of the track, early maintenance and some precautions can be taken to the specific section. This work contributes to existing knowledge of track stiffness measurement by providing a straightforward implementation, time-saving, and cost-efficiency method. There is a limitation that the model is developed based on a simulated dataset with three irregularities considered. More irregularities will be included in the simulated dataset, and the field data is required to test the model's performance in the future.

APPENDIX

The three values in the number of convolutional filters are for three different layers.

TABLE 4. Optimal hyperparameters for three window sizes.

Hyperparameter	250	500	1000
The number of convolutional filters	• 222 • 152 • 197	• 132 • 237 • 112	• 197 • 42 • 147
The size of the dense layers	147	112	142
The dropout rates	0.5	0.5	0.5
Learning rate	0.003	0.0004	0.0002
Batch size	8	8	8
Activation function	Relu	Relu	Relu
Optimizer	Adam	Adam	Adam
Momentum	N/A	N/A	N/A

ACKNOWLEDGMENT

The authors would like to acknowledge the assistance from LORAM, Brazilian Railway Authority, China Academy of Railway Sciences (CARS), Network Rail, and Rail Safety and Standards Board (RSSB), U.K. The APC has been sponsored by the University of Birmingham Library's Open Access

Fund. The authors also wish to thank the European Commission for the financial sponsorship of the H2020-MSCA-RISE Project no.691135 ''RISEN: Rail Infrastructure Systems Engineering Network'', which enables a global research network that addresses the grand challenge of railway infrastructure resilience and advanced sensing in extreme environments (www.risen2rail.eu).

REFERENCES

[1] A. L. Pita, P. F. Teixeira, and F. Robusté, ''High speed and track deterioration: The role of vertical stiffness of the track,'' *Proc. Inst. Mech. Eng. F, J. Rail Rapid Transit*, vol. 218, no. 1, pp. 31–40, Jan. 2004.
[2] W. E. Ebersöhn, ''Substructure influence on track maintenance requirements,'' Dept. Civil Environ. Eng., Univ. Massachusetts, Amherst, MA, USA, Geotech. Rep. AAR95-423D, Feb. 1995.
[3] W. Ebersöhn and E. T. Selig, ''Track modulus measurements on a heavy haul line,'' *Transp. Res. Rec.*, vol. 1470, no. 1470, p. 73, 1994.
[4] E. Berggren, Å. Jahlénius, and B. E. Bengtsson, ''Continuous track stiffness measurement: An effective method to investigate the structural conditions of the track,'' in *Proc. Railway Eng. Conf.*, London, U.K., Jul. 2002.
[5] P. Wang, L. Wang, R. Chen, J. Xu, J. Xu, and M. Gao, ''Overview and outlook on railway track stiffness measurement,'' *J. Mod. Transp.*, vol. 24, no. 2, pp. 89–102, Jun. 2016.
[6] A. D. Kerr, ''On the determination of the rail support modulus k,'' *Int. J. Solids Struct.*, vol. 37, no. 32, pp. 4335–4351, Aug. 2000.
[7] G. Zhang, ''Research on right level of track structure stiffness and trackpart stiffness,'' *China Railway Sci.*, vol. 23, no. 1, pp. 51–57, 2002.
[8] E. Berggren, ''Railway track stiffness—Dynamic measurements and evaluation for effective maintenance,'' Ph.D. thesis, Roy. Inst. Technol. (KTH), Stockholm, Sweden, 2009.
[9] S. Kaewunruen and A. Remennikov, ''Applications of experimental modal testing for estimating dynamic properties of structural components,'' in *Proc. Austral. Struct. Eng. Conf.*, Newcastle, VIC, Australia, 2005.
[10] S. Kaewunruen and A. Remennikov, ''Monitoring structural degradation of rail bearing pads in laboratory using impact excitation technique,'' in *Proc. 1st Int. Conf. Struct. Condition Assessment; Monit. Improvement*, Perth, WA, Australia, Dec. 2005, pp. 399–405.
[11] M. Hosseingholian, M. Froumentin, and A. Robinet, ''Dynamic track modulus from measurement of track acceleration by portancemetre,'' in *Proc. 9th World Congr. Railway Res. (WCRR)*, Lille, France, May 2011, p. 12.
[12] D. Li, R. Thompson, and S. Kalay, ''Development of continuous lateral and vertical track stiffness measurement techniques,'' in *Proc. Railway Eng.*, London, U.K., 2002.
[13] M. P. N. Burrow, A. H. C. Chan, and A. Shein, ''Deflectometer-based analysis of ballasted railway tracks,'' *Proc. Inst. Civil Eng., Geotech. Eng.*, vol. 160, no. 3, pp. 169–177, Jul. 2007.
[14] W. Wangqing, Z. Geming, Z. Kaiming, and L. Lin, ''Development of inspection car for measuring railway track elasticity,'' in *Proc. 6th Int. Heavy Haul Conf.*, Cape Town, South Africa, 1997.
[15] P. Quirke, D. Cantero, E. J. O'Brien, and C. Bowe, ''Drive-by detection of railway track stiffness variation using in-service vehicles,'' *Proc. Inst. Mech. Eng. F, J. Rail Rapid Transit*, vol. 231, no. 4, pp. 498–514, Apr. 2017.
[16] M. Mehrali, M. Esmaeili, and S. Mohammadzadeh, ''Application of data mining techniques for the investigation of track geometry and stiffness variation,'' *Proc. Inst. Mech. Eng. F, J. Rail Rapid Transit*, vol. 234, no. 5, pp. 439–453, May 2020.
[17] Z. Cai, G. P. Raymond, and R. J. Bathurst, ''Natural vibration analysis of rail track as a system of elastically coupled beam structures on Winkler foundation,'' *Comput. Struct.*, vol. 53, no. 6, pp. 1427–1436, Dec. 1994.
[18] D. M. Steffens, ''Identification and development of a model of railway track dynamic behaviour,'' M.S. thesis, School Built Environ., Queensland Univ. Technol., Brisbane, QLD, Australia, 2005.
[19] J. Leong, ''Development of a limit state design methodology for railway track,'' M.S. thesis, School Civil Eng., Queensland Univ. Technol., Brisbane, QLD, Australia, 2007.
[20] D. Li, C. Ngamkhanong, and S. Kaewunruen, ''Time-dependent topology of railway prestressed concrete sleepers,'' *IOP Conf. Ser., Mater. Sci. Eng.*, vol. 245, Oct. 2017, Art. no. 032046.
[21] S. Pouyanfar, S. Sadiq, Y. Yan, H. Tian, Y. Tao, M. P. Reyes, M.-L. Shyu, S.-C. Chen, and S. S. Iyengar, ''A survey on deep learning: Algorithms, techniques, and applications,'' *ACM Comput. Surv.*, vol. 51, no. 5, pp. 1–36, 2018.
[22] J. Sresakoolchai and S. Kaewunruen, ''Detection and severity evaluation of combined rail defects using deep learning,'' *Vibration*, vol. 4, no. 2, pp. 341–356, Apr. 2021.
[23] O. Avci, O. Abdeljaber, S. Kiranyaz, M. Hussein, M. Gabbouj, and D. J. Inman, ''A review of vibration-based damage detection in civil structures: From traditional methods to machine learning and deep learning applications,'' *Mech. Syst. Signal Process.*, vol. 147, Jan. 2021, Art. no. 107077.
[24] H. Tsunashima, ''Condition monitoring of railway tracks from car-body vibration using a machine learning technique,'' *Appl. Sci.*, vol. 9, no. 13, p. 2734, 2019.
[25] S. Albawi, T. A. Mohammed, and S. Al-Zawi, ''Understanding of a convolutional neural network,'' in *Proc. Int. Conf. Eng. Technol. (ICET)*, Aug. 2017, pp. 1–6.
[26] O. Banos, J.-M. Galvez, M. Damas, H. Pomares, and I. Rojas, ''Window size impact in human activity recognition,'' *Sensors*, vol. 14, no. 4, pp. 6474–6499, Apr. 2014.
[27] A. Jain, K. Nandakumar, and A. Ross, ''Score normalization in multimodal biometric systems,'' *Pattern Recognit.*, vol. 38, no. 12, pp. 2270–2285, Dec. 2005.
[28] L.-C. Chen, G. Papandreou, I. Kokkinos, K. Murphy, and A. L. Yuille, ''DeepLab: Semantic image segmentation with deep convolutional nets, atrous convolution, and fully connected CRFs,'' *IEEE Trans. Pattern Anal. Mach. Intell.*, vol. 40, no. 4, pp. 834–848, Apr. 2017.
[29] H. Meng, T. Yan, F. Yuan, and H. Wei, ''Speech emotion recognition from 3D log-mel spectrograms with deep learning network,'' *IEEE Access*, vol. 7, pp. 125868–125881, 2019.
[30] X. Lei, H. Pan, and X. Huang, ''A dilated CNN model for image classification,'' *IEEE Access*, vol. 7, pp. 124087–124095, 2019.
[31] L.-C. Chen, G. Papandreou, F. Schroff, and H. Adam, ''Rethinking atrous convolution for semantic image segmentation,'' 2017, *arXiv:1706.05587*.
[32] M. Hosseingholian, M. Froumentin, and D. Levacher, ''Continuous method to measure track stiffness a new tool for inspection of rail infrastructure,'' *World Appl. Sci. J.*, vol. 6, no. 5, pp. 579–589, 2009.
[33] L. Puzavac and Z. Popović, ''Vertical track geometry deterioration modeling,'' *Izgradnja*, vol. 64, nos. 1–2, pp. 7–20, 2010.
[34] T. R. Sussman, W. Ebersöhn, and E. T. Selig, ''Fundamental nonlinear track load-deflection behavior for condition evaluation,'' *Transp. Res. Rec., J. Transp. Res. Board*, vol. 1742, no.s 1, pp. 61–67, Jan. 2001.

JUNHUI HUANG received the bachelor's degree in electrical and railway engineering and the master's degree in railway systems engineering and integration from the University of Birmingham, U.K., where he is currently pursuing the Ph.D. degree. His research interest includes artificial intelligent applied in railway.

XIAOJIE YIN received the bachelor's degree in civil engineering from the Inner Mongolia University of Science and Technology, in 2020, and the master's degree from the University of Birmingham, in 2021. His research interest includes machine learning application in public transport.

SAKDIRAT KAEWUNRUEN received the Ph.D. degree in structural engineering from the University of Wollongong, Australia. He has expertise in transport infrastructure engineering and management and successfully dealing with all stages of infrastructure life cycle and assuring safety, reliability, resilience, and sustainability of rail infrastructure systems. He is a Chartered Engineer. He has over 400 technical publications.